ELSEVIER

International Journal of Biological Macromolecules 41 (2007) 447–453

INTERNATIONAL JOURNAL OF
Biological
Macromolecules
STRUCTURE, FUNCTION AND INTERACTIONS

www.elsevier.com/locate/ijbiomac

Haloadaptation: Insights from comparative modeling studies of halophilic archaeal DHFRs

Panagiotis L. Kastritis, Nikos C. Papandreou, Stavros J. Hamodrakas *

Department of Cell Biology and Biophysics, Faculty of Biology, University of Athens, Panepistimiopolis, Athens 157 01, Greece

Received 2 April 2007; received in revised form 13 June 2007; accepted 13 June 2007
Available online 19 June 2007

Abstract

Proteins of halophilic archaea function in high-salt concentrations that inactivate or precipitate homologous proteins from non-halophilic species. Haloadaptation and the mechanism behind the phenomenon are not yet fully understood. In order to obtain useful information, homology modeling studies of dihydrofolate reductases (DHFRs) from halophilic archaea were performed that led to the construction of structural models. These models were subjected to energy minimization, structural evaluation and analysis. Complementary approaches concerning calculations of the amino acid composition and visual inspection of the surfaces and cores of the models, as well as calculations of electrostatic surface potentials, in comparison to non-halophilic DHFRs were also performed. The results provide evidence that sheds some light on the phenomenon of haloadaptation: DHFRs from halophilic archaea may maintain their fold, in high-salt concentrations, by sharing highly negatively charged surfaces and weak hydrophobic cores.

Keywords: DHFR; Extremophiles; Halophiles; Archaea; Homology (comparative) modeling; Haloadaptation

1. Introduction

Microorganisms that are adapted to living under extreme saline conditions have been found in many hypersaline environments, such as in the Dead Sea and in the Great Salt Lake, Utah [1]. In order to survive at high-salt concentrations these microorganisms have to maintain an osmotic balance with their external environment. The halophilic archaea accumulate high concentrations of KCl in their cytoplasm up to 4 M [1].

Dihydrofolate reductase (DHFR) is an excellent model system with which to examine the halophilic adaptation of enzymes from the extremely halophilic archaea. Dihydrofolate reductase (DHFR; E.C. 1.5.1.3) is the NADPH-dependent enzyme that catalyzes the reduction of 7,8-dihydrofolic acid to tetrahydrofolic acid, a reaction essential in thymidine biosynthesis. The strategic role of DHFR in cell metabolism led to the development of an enormous amount of potent inhibitors of the enzyme, following the observation that blocking of the enzymatic activity of DHFR leads to cell death, due to the stoppage of folate regeneration and lack of its analogues [2]. Therefore, DHFR is used as a target for various anti-neoplasmic, anti-bacterial, anti-fungal and anti-malarial drugs [2]. The study of DHFRs from halophilic archaea is important for the development of proteins with novel properties, because through the understanding of their folds, conclusions may be drawn about the structural features that underlie their unique feature of haloadaptation.

Two controversial theories exist in order to interpret the halophilic adaptation mechanism: Either high ionic strength conditions stabilize the proteins through the interaction of a few key ions and large water networks [3], or, acidic, highly ionic surfaces and weak hydrophobic cores act as balancing factors of the endogenous capability of these proteins to maintain their fold in extreme salt concentrations [4]. Only a single structure of a halophilic archaeal DHFR from the organism *Halobacterium volcanii* (*hv*DHFR, PDB ID: 1VDR [5]) has experimentally been determined (Fig. 1) [1]. The architecture of the enzyme is very similar to the non-halophilic DHFRs. It consists of a mixed β-pleated sheet, with eight β-strands that form the core of the enzyme, surrounded by four α-helices and several loops. *Hv*DHFR was crystallized as a dimer and exhibits an rmsd deviation of 0.6 Å between the two chains, mainly due to the presence of an α-helix in one of them and the absence of this structural

* Corresponding author. Tel.: +30 210 7274931; fax: +30 210 7274254.
E-mail address: shamodr@biol.uoa.gr (S.J. Hamodrakas).

0141-8130/$ – see front matter © 2007 Elsevier B.V. All rights reserved.
doi:10.1016/j.ijbiomac.2007.06.005

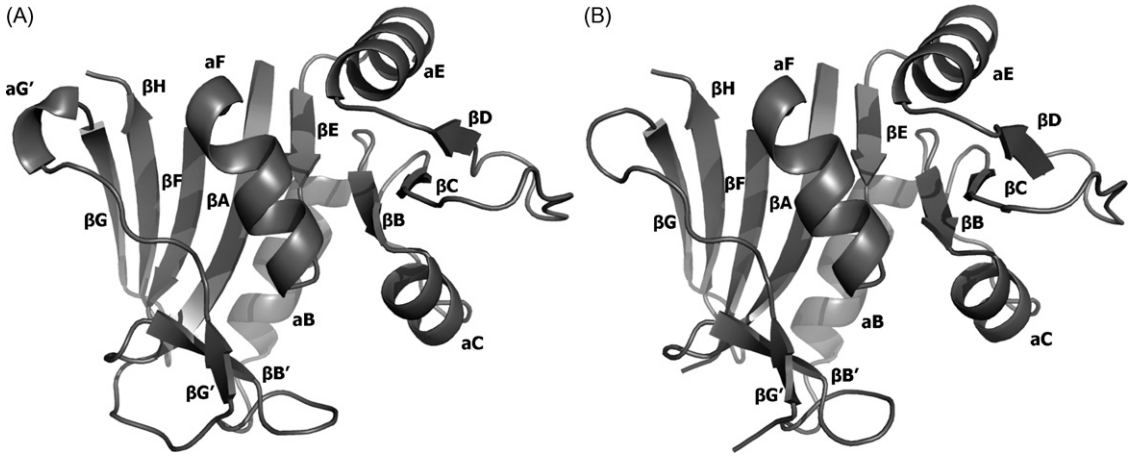

Fig. 1. Cartoon representation generated with PyMOL [6], illustrating chain A (A) and chain B (B) of the crystal structure of *Halobacterium volcanii* DHFR [1]. The labeling of secondary structure elements was made following [2]. Structural alignment of the two chains was performed utilizing the CE (combinatorial extension) method [7] and indicates an rmsd deviation of 0.6 Å between the two chains, mainly due to the presence of an α-helix in one of them (aG′ in chain A), and the absence of this structural element in the other (chain B).

element in the other. In other DHFRs that were crystallized as dimers, such difference does not exist.

In this work, homology (comparative) modeling studies of DHFRs from halophilic archaea were performed, in order to identify distinct structural features in proteins of halophilic organisms that may shed some light on haloadaptation mechanisms. If such features are found they may also provide useful clues for the design of resistant proteins under high-salt concentrations.

2. Materials and methods

2.1. Data mining and calculation of the amino acid composition of DHFRs

Several methods were combined in order to construct, evaluate and analyze three-dimensional model structures from halophilic archaeal DHFRs. Seven DHFR sequences from four organisms (*Haloarcula marismortui, Halobacterium volcanii, Haloquadratum walsbyi* and *Natrosomonas pharaonis*) were retrieved from UNIPROT 9.1 [8]. The genome of the strain ATCC 43049 of *Haloarcula marismortui* contains two genes that encode for DHFR. *Halobacterium volcanii* genome also contains two genes (folA and hdrB) that encode for DHFR. *Haloquadratum walsbyi* encodes two genes that encode for two different DHFRs from two locuses, named HQ2455A and HQ1842A. Amino acid composition was calculated for each sequence separately and the average values from all seven halophilic archaeal sequences were compared to the average amino acid composition of all other DHFR sequences that are deposited in UNIPROT, utilizing MEGA 3.1 [9]. This set includes 568 DHFR sequences from various organisms: 522 DHFRs belong to bacterial species, 29 to the fungal group and 17 to the metazoan group. DHFR sequences from the plant and the protozoan groups were not considered, because DHFRs of these species are linked with thymidylate synthase. Relative hydrophobic values of polar and non-polar amino acids that are found in DHFRs were calculated, multiplying the percentage of the average amino acid composition of DHFRs and the value assigned to each amino acid separately, according to the normalized consensus hydrophobicity scale implemented by Eisenberg et al. [10]. The numerical values used, were taken from the consensus scale of Eisenberg et al. [11], normalized so that the mean value of the hydrophobicities is zero and the standard deviation is unity. The Eisenberg hydrophobicity scale is a consensus set of values that approximates the free energy of transfer of the side chain of the amino acid from water to an apolar environment.

2.2. Construction, evaluation, refinement and selection of the models

The sequences of the seven halophilic archaeal DHFRs obtained from UNIPROT 9.1 were given as input in TASSER-lite [12], a threading server that is optimized for modeling homologous protein sequences with an identity greater than 35% with respect to a known template. The template for the modeling of the query sequence is identified using the threading program PROSPECTOR_3 [13] and the structure is refined using the Threading-ASSembly-Refinement (TASSER) program [14]. Models that were derived from TASSER-lite lack some residues, which are located either on the surface or the cores of the enzymes. In order to complete the models, MODELLER 8v1 [15] was used. An alternative approach for the construction of the structural models of halophilic archaeal DHFRs, incorporated the use of MODELLER only, where the sequence and the experimentally determined structure of *Haloferax volcanii (hv)* DHFR (1VDR, chain A) [1] acted as template. Pairwise sequence alignments were performed with CLUSTALW [16], between each available halophilic DHFR sequence and the sequence of *hv*DHFR (Uniprot accession no: P15093). Output files that were generated in pir format were provided as input to MODELLER 8v1 (Table 1).

Pairwise structural alignments between the models that were derived from TASSER-lite and MODELLER, as well as visual

Table 1
Amino acid sequences of halophilic archaeal species used for comparative modeling

Uniprot accession number	Sequence length	Halophilic archaeal species
Q9UWQ4	194	*Halobacterium volcanii*
P15093	162	*Halobacterium volcanii*
Q5V3R2	185	*Haloarcula marismortui*
Q5V600	167	*Haloarcula marismortui*
Q3IQP3	165	*Natrosomonas pharaonis*
Q18HG9	195	*Haloquadratum walsbyi*
Q18J41	160	*Haloquadratum walsbyi*

Accession numbers were taken from Uniprot [8].

inspection were performed to identify if these models share the same fold. The derived models from both methodologies were energetically unfavourable. In order to refine the models energy minimization was performed, utilizing the subroutine '*Minimize*' of TINKER [17], applying CHARMM27 force fields [18], with an rmsd gradient per atom criterion of 4 Å. The refined molecules were checked with WHAT_CHECK [19] and Ramachandran plots were constructed utilizing PROCHECK [20]. After each step, the models were visually inspected with the graphics program O [21].

At this stage, it should perhaps be mentioned that, the experimentally determined structure of *H. volcanii* was modelled too, by both procedures, in order to act as test case.

A close comparison of the models derived from the TASSER-lite and MODELLER only procedures described above, indicates that the models derived by the latter procedure appear to be more realistic: compared to the experimentally determined structure of *H. volcanii* [1], they exhibit significantly lower rmsd values than the models derived by the former procedure (data not shown and Table 2). For this reason, the models derived utilizing MODELLER only were selected for further structural analysis.

2.3. Structural analysis of halophilic archaeal DHFRs

Pairwise superposition of the models was performed to identify structural resemblances, utilizing PyMOL v0.99 (Table 2) [6]. The average length of the β-strands of the molecules was calculated utilizing DSSP [22] and was compared to the average length of 10 experimentally determined DHFR structures. These 10 DHFRs belong to the species *Candida albicans, Escherichia coli, Gallus gallus, Homo sapiens, Lactobacillus casei, Mus musculus, Mycobacterium tuberculosis, Pneumocystis carinii, Plasmodium vivax and Rattus norvegicus*, corresponding to the PDB IDs 1M7A (chain A), 7DFR, 1DR1, 1KMV, 3DFR, 1U70 (chain A), 1DG5, 1DAJ, 2BL9 (chain A) and 1KLK, respectively. Measurement of the average number of charged residues that lie on the surface of the models was performed and compared to the average number of the charged residues that lie on the surface of the above-mentioned 10 DHFR structures, excluding *Plasmodium vivax* DHFR from the set, in which large segments located on the surface are missing. In order to locate charged residues (Arg, Lys, Asp, Glu, His) that lie on the surface, PyMol's subroutine '*surface*' was implemented, after selecting each charged residue for each DHFR. This subroutine calculates the Connolly surface [23] of the selected residue. Residues that lack this surface were considered internal, whereas all other residues that formed a Connolly surface, were considered to lie on the surface of the molecules. Clearly, this was manual selection taking into account that a Connolly surface is defined only for exposed residues. This procedure was applied to the crystallographicaly determined structures of the *H. volcanii* DHFR, the seven halophilic archaeal models and the nine homologous experimentally determined DHFRs from different non-halophilic organisms that were retrieved from PDB (see above). The total average number for each surfacial charged residue was calculated for the three sets, applying this procedure.

Electrostatic surface potentials for all models were calculated with GRASP [24] in order to be compared to surface potentials from three non-halophilic experimentally determined DHFRs: human (*h*DHFR, PDB ID: 1KMV); *Escherichia coli* (*ec*DHFR, PDB ID: 7DFR) and *Candida albicans* (caDHFR, PDB ID: 1M7A). In addition, structural alignment of the models with the non-halophilic DHFR, *h*DHFR, (PDB ID: 1DHF, chain A) was done, utilizing PyMOL v0.99 [6], to compare the cores of the structures. The number of potential hydrogen bonds and salt bridges in the structural models of the halophilic archaeal DHFRs was calculated utilizing the WHAT IF server [25] and compared to that of DHFRs from non-halophilic species. In the WHAT IF server, a salt bridge is defined as the interaction between a negative atom (side chain oxygens in Asp or Glu) and

Table 2
Pairwise superposition, implemented with PyMOL v0.99 [6], between the final models obtained after comparative modeling, and the experimentally determined structure of *Halobacterium volcanii* (PDB ID 1VDR, chain A) [1]

–	Q9UWQ4 1	P15093 2	Q5V3R2 3	Q5V600 4	Q3IQP3 5	Q18HG9 6	Q18J41 7	1VDR 8
1	–	1.334	3.544	0.831	1.050	3.325	1.334	1.289
2	126	–	0.813	0.680	0.805	0.885	0.740	0.640
3	144	138	–	1.566	1.435	2.325	1.380	1.190
4	134	151	130	–	0.810	1.362	0.580	0.500
5	132	125	136	145	–	1.473	0.750	0.685
6	154	137	141	133	136	–	1.280	1.190
7	126	159	149	147	136	131	–	0.250
8	121	157	144	150	124	145	156	–

Left and right halves of the table, indicate the number of C_α atoms aligned in each superposition and rmsd values in Å, respectively.

a positive atom (side chain nitrogens in Arg, Lys or His) with an interatomic distance less than 7.0 Å. His is considered positively charged. In our procedure, the cut-off for the interatomic distance was set to 5.0 Å, and His was considered both neutral and charged. The '*Hydrogen bond*' module of WHAT IF [25] computes all possible hydrogen bonds in a protein structure.

3. Results and discussion

3.1. Amino acid composition of DHFRs of halophilic archaea reveals certain characteristics

DHFR sequences of halophilic archaea exhibit certain differences compared to DHFR sequences from non-halophilic species (Fig. 2a). It is clearly observed that there is an increased percentage of acidic residues, such as Glu (8.8%) and Asp (8.4%), compared to the overall percentage concerning DHFRs from other taxa (6.9% and 5.4%, respectively). In total, the average percentage of negatively charged residues in halophilic archaeal DHFRs (17.2%) is significantly higher than that calculated from the other taxa (12.3%). The enrichment in Asp and Glu residues in halophilic archaeal DHFRs relative to mesophilic

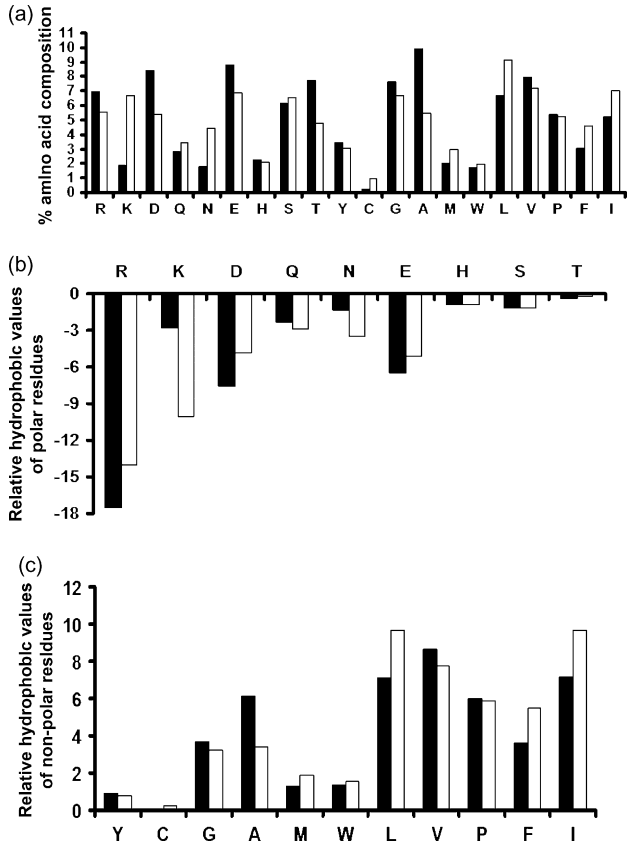

Fig. 2. Column charts indicating (a) the percentage of the average amino acid composition of DHFRs. The black bar corresponds to halophilic archaeal species and the white bar corresponds to the average amino acid composition of all other groups except the halophilic archaeal group. These groups include bacterial, fungal and the metazoan taxa. (b) and (c) charts depict the relative hydrophobic values of polar and non-polar amino acids that are found in DHFRs (see text). Black and white bars correspond to residues that are found in halophilic archaeal DHFRs and non-halophilic DHFRs, respectively.

DHFRs has been previously observed, comparing the amino acid composition of *H. volcanii* DHFR to that of *E. coli* and *L. casei* [1,27]. However, as these authors point out, the three-dimensional arrangement of the acidic residues into clusters on the protein surface may be more relevant to stability of the halophilic proteins in high-salt concentrations, than the absolute numbers of acidic residues. An abundance of alanines is also observed (9.9% in comparison to an average of 5.5% from other taxa). Hydrophilic residues, according to the Eisenberg normalized consensus hydrophobicity scale [10], are dominant in the sequences of halophilic archaeal DHFRs in comparison to DHFRs from other taxa (Fig. 2b). Lysine is a notable exception to the observed dominance and this is discussed further below and in detail, for the first time, in the glutamate dehydrogenase structure in [28]. The observed overall low percentage in large hydrophobic amino acids, such as Ile and Phe, and the relative increase of small hydrophobic residues, such as alanines, according to the Eisenberg hydrophobicity scale (Fig. 2c), may imply that residues lying in the core of the enzyme probably form a less stable hydrophobic core compared to the core from non-halophilic species (see also below). Moreover, the reduced percentage of positively charged residues such as lysine and arginine (8.8% overall) in halophilic archaeal DHFRs, compared to the overall average percentage (12.2%) in non-halophilic species, probably suggests that a rich and extended salt bridge network within the halophilic proteins is more difficult to be formed than in non-halophilic ones. The difference between the above-mentioned percentages does not change if His is considered as charged because its percentage is more or less equal in DHFRs from halophilic archaeal DHFRs and non-halophilic ones (2.3% and 2.1%, respectively). A notable aspect of the amino acid sequences of halophilic DHFRs is that they exhibit a clear enrichment of Arg residues compared with Lys residues (Fig. 2a and b). This, has also been observed previously [1 and Refs. therein] and, as Pieper et al. point out, may be related to the fact that Arg side chains tend to bind more water molecules than lysine side chains, which is well documented by an analysis of the distributions of water molecules around well ordered residues in high resolution crystal structures [29].

In general, it should be noted that these trends in amino acid composition have already been noticed and discussed in an excellent way by previous authors [1,27]. However, they are clearly exemplified and much more pronounced in this study, which has the advantage to include many more sequences of halophilic archaeal DHFRs.

3.2. Structural differences between halophilic archaeal DHFRs and non-halophilic DHFRs

The average length of the β-strands of the halophilic archaeal structural models was calculated utilizing DSSP [22] and compared to the average length of ten experimentally determined mesophilic DHFR structures. Structural analysis of the constructed models showed that DHFRs of halophilic archaea adopt a narrower β-pleated sheet than mesophilic DHFRs with crystallographicaly determined structures (Fig. 3a). Due to the fact that the β-pleated sheet acts as the core of the enzyme, it is

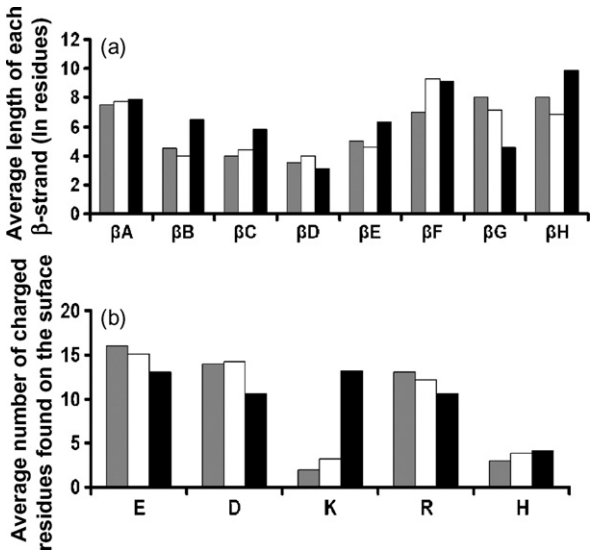

Fig. 3. Bar charts depicting (a) The average length in residues of each β-strand separately and (b) the average number of charged residues found on the surface of the molecules. White and black bars correspond to halophilic archaeal and non-halophilic DHFRs, respectively, whereas the gray bar corresponds to the crystallographicaly determined structure of *Halobacterium volcanii* DHFR [1].

suggested that its shape and length of its strands may provide these proteins with structural features that reinforce haloadaptation. The only two strands of the narrower β-pleated sheet of the halophilic archaeal DHFR, that are longer than those that correspond to non-halophilic DHFRs, are strands that lie on the surface of the molecule (strands βD and βG).

Furthermore, the increased average number of negatively charged residues that are located on the surface (29.3) and the decreased overall average number of positively charged residues (15.4 – and if His is considered positive, 19.3) on the surface of the resulted models, in comparison to 9 mesophilic homologous structures that were experimentally determined, may be connected to the fact that halophilic proteins maintain their fold in high-salt concentrations. Interestingly, the average number of Glu and Asp that lie on the surface of mesophilic homologous DHFR structures is slightly lower (23.6), but the average number of positively charged residues on the surface of mesophilic DHFRs is much higher (24.7 – and if His is considered positive, 28.8). A comparison of the average numbers of charged residues that lie on the surfaces of halophilic and mesophilic molecules is shown in Fig. 3b.

Relative electrostatic surface potentials of the models, calculated with GRASP [24], clearly reveal that the surfaces of the halophilic models are highly acidic compared to the non-halophilic DHFRs (Fig. 4). Only the DHFR from the halophilic *Haloquadratum walsbyi* (Fig. 4c and d) seems to divert from the observations, and this is probably due to the different habitat of this species: it does not live in the Dead Sea like all other species, but it is located in salt crystals, where there is almost total lack of water molecules and different mechanisms seem to maintain the folds of its proteins in this extreme environment [26]. The presence of clusters of non-interacting negatively charged residues has been observed in the crystal structure of *Haloferax volcanii* [1]. Such clusters are most probably associated with unfavorable electrostatic energy at low-salt concentrations, and may account for the instability of *hv*DHFR at salt concentrations lower than 0.5 M [1]. Presuwably, they help to stabilize the protein by competing with the salt for hydration at higher salt concentrations [30].

Studies of a number of other halophilic enzymes have clearly shown that a dominant structural feature of halophilic proteins is an outer shell of negatively charged residues [3,28,31–33]. Furthermore, mutation studies of surface residues, in the enzyme malate dehydrogenase have been performed [34,35] and their effect on the halophilic behaviour and other biochemical properties of this enzyme have been examined.

Potential salt bridges computed for non-halophilic and halophilic DHFRs (Table 3) do not show significant trends, most probably indicating that a large network of these intramolecular interactions does not occur. Also, putative hydrogen bonds within halophilic archaeal molecules are similar in number to their non-halophilic counterparts; thus, apparently, an extremely large network of hydrogen bonds within the halophilic molecules does not prevail (Table 3).

It is true that conclusions drawn from homology-based structural models of halophilic enzymes should be considered with great caution [36]. For example, acidic clusters modelled in *hv*DHFR and postulated to contribute to low-salt instability through charge repulsion [37] were found not to be in elec-

Table 3
Calculated intramolecular salt bridges and hydrogen bonds, with WHAT IF [25], from the DHFR structures of three non-halophilic species (in bold) and the seven structural models of halophilic species, derived by comparative modelling

Organism	Sequence length	Salt bridges (1)	Salt bridges (2)	Hydrogen bonds
Escherichia coli	**159**	**13**	**17**	**113**
Homo sapiens	**186**	**19**	**23**	**139**
Candida albicans	**192**	**34**	**36**	**168**
Halobacterium volcanii	194	20	32	100
Halobacterium volcanii	*162*	28	28	108
Haloarcula marismortui	185	38	43	111
Haloarcula marismortui	*167*	10	11	111
Natronomonas pharaonis	165	19	20	96
Haloquadratum walsbyi	195	14	18	115
Haloquadratum walsbyi	*160*	17	17	112

Salt bridges were calculated using a reduced distance cut-off (5 Å, see text) and His residues were considered both as neutral (1) and charged (2).

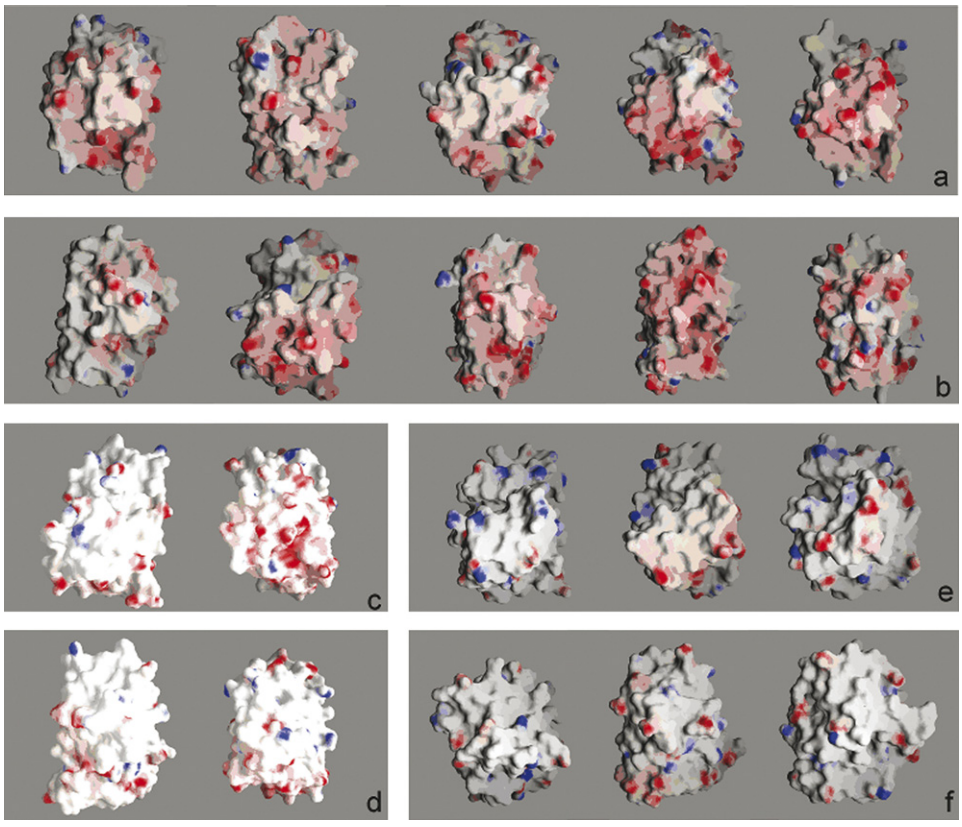

Fig. 4. Relative electrostatic surface potentials of the models, calculated with GRASP [24]. It is clearly observed that all archaeal DHFRs of species that live in the Dead Sea (a and b) exhibit highly negatively charged surfaces. Only the DHFR from *Haloquadratum walsbyi* seems to differ (c and d) due to the extreme environment where this organism lives [26]. From left to right, halophilic enzymes correspond to sequences with Uniprot [8] accession numbers Q5V600, Q5V3R2, P15093, Q9UWQ4, Q3IQP3 (a and rear view, b), Q18J41 and Q18HG9 (c and rear view, d). Non-halophilic DHFRs represented herein, correspond to (from left to right) the apoenzymes of human DHFR (PDB ID: 1KMV), *Escherichia coli* DHFR (PDB ID: 7DFR) and *Candida albicans* DHFR (PDB ID: 1M7A) (e and rear view, f).

trostatic interaction when the crystal structure was solved [1]. Further, halophilic proteins cannot be considered simply as well-folded polypeptide chains interacting with each other in a high-salt environment. They are, in fact, complexes of proteins and solvation shells, which inherently include specific interactions between salt ions, water molecules and polypeptides; these interactions determine solubility, stabilization and interactions of subunits. However, data obtained even from model structures cannot be ignored because they may well represent essential features important for haloadaptation.

4. Conclusions

Comparisons of the amino acid composition and sequences of homologous DHFRs from mesophilic and halophilic organisms revealed major differences. The most profound difference in halophilic DHFRs is a general increase in the content of acidic residues, Asp and Glu, and a decrease in the content of basic residues, particularly Lys. Another striking but perhaps more important difference is a decrease in the overall hydrophobic content of the halophilic proteins. Model structures of the halophilic DHFRs indicate that the hydrophobic cores of these proteins are smaller (the degree of hydrophobicity is decreased) and that highly negatively charged surfaces prevail. Therefore, we propose that the mechanism of haloadaptation of DHFRs from halophilic archaea involves the presence of presumably highly negatively charged, surfaces and weak hydrophobic cores that act as balancing factors of the capability of these proteins to maintain their fold. These findings are clearly in favour to one of the theories that have been proposed to interpret halophilic adaptation mechanisms [4]. However, detailed, high resolution X-ray and/or NMR structures in the presence of high and low-salt concentrations and water are needed to reveal the exact details of the haloadaptation mechanisms.

Acknowledgements

We thank the University of Athens for financial support. We thank the reviewers of this manuscript for their useful comments.

Appendix A. Supplementary data

Supplementary data associated with this article can be found, in the online version, at doi:10.1016/j.ijbiomac.2007.06.005.

References

[1] U. Pieper, G. Kapadia, M. Mevarech, O. Herzberg, Structure 6 (1998) 75.
[2] R.L. Blakley, Adv. Enzymol. Relat. Areas Mol. Biol. 70 (1995) 23.
[3] S.B. Richard, D. Madern, E. Garcin, G. Zaccai, Biochemistry 39 (2000) 992.

[4] M. Mevarech, F. Frolow, L.M. Gloss, Biophys. Chem. 86 (2000) 155.
[5] A. Kouranov, L. Xie, J. de la Cruz, L. Chen, J. Westbrook, P.E. Bourne, H.M. Berman, Nucleic Acids Res. 34 (2006) D302.
[6] W.L. DeLano, The PyMOL Molecular Graphics System, DeLano Scientific, San Carlos, CA, US, 2002 (http://www.pymol.org).
[7] I.N. Shindyalov, P.E. Bourne, Protein Eng. 11 (1998) 739.
[8] A. Bairoch, R. Apweiler, C.H. Wu, W.C. Barker, B. Boeckmann, S. Ferro, E. Gasteiger, H. Huang, R. Lopez, M. Magrane, M.J. Martin, D.A. Natale, C. O'Donovan, N. Redaschi, L.S. Yeh, Nucleic Acids Res. 33 (2005) D154.
[9] S. Kumar, K. Tamura, M. Nei, Brief Bioinform. 5 (2004) 150.
[10] D. Eisenberg, E. Schwarz, M. Komarony, R. Wall, J. Mol. Biol. 179 (1984) 125.
[11] D. Eisenberg, R.M. Weiss, T.C. Terwilliger, W. Wilcox, Faraday Symp. Chem. Soc. 17 (1982) 109.
[12] S.B. Pandit, Y. Zhang, J. Skolnick, Biophys. J. 91 (2006) 4180.
[13] J. Skolnick, D. Kihara, Y. Zhang, Proteins 56 (2004) 502.
[14] Y. Zhang, J. Skolnick, Proc. Natl. Acad. Sci. USA 101 (2004) 7594.
[15] A. Sali, T. Blundell, J. Mol. Biol. 234 (1993) 779.
[16] J.D. Thompson, D.G. Higgins, T.J. Gibson, Nucleic Acids Res. 22 (1994) 4673.
[17] J.W. Ponder, D.A. Case, Adv. Prot. Chem. 66 (2003) 27.
[18] N. Foloppe, A.D. MacKerell Jr., J. Comput. Chem. 21 (2000) 86.
[19] R.W. Hooft, G. Vriend, C. Sander, E.E. Abola, Nature 381 (1996) 272.
[20] R.A. Laskowski, M.W. MacArthur, D.S. Moss, J.M. Thornton, J. Appl. Cryst. 26 (1993) 283.
[21] T.A. Jones, J.Y. Zou, S.W. Cowan, M. Kjeldgaard, Acta Cryst. A 47 (1991) 110.
[22] W. Kabsch, C. Sander, Biopolymers 22 (12) (1983) 2577.
[23] M.L. Connolly, Science 221 (1983) 709.
[24] A. Nicholls, K.A. Sharp, B. Honig, Proteins 11 (1991) 281.
[25] G. Vriend, J. Mol. Graph. 8 (1990) 52.
[26] H. Bolhuis, P. Palm, A. Wende, M. Falb, M. Rampp, F. Rodriguez-Valera, F. Pfeiffer, D. Oesterhelt, BMC Genomics 7 (2006) 169.
[27] D.B. Wright, D.D. Banks, J.R. Lohman, J.L. Hilsenbeck, L.M. Gloss, J. Mol. Biol. 323 (2002) 327.
[28] K.L. Britton, T.J. Stillman, K.S.P. Yip, P. Forterre, P.C. Engel, D.W. Rice, J. Biol. Chem. 273 (1998) 9023.
[29] N. Thanki, J.M. Thornton, J.M. Goodfellow, J. Mol. Biol. 202 (1988) 637.
[30] J.K. Lanyi, Bacteriol. Rev. 38 (1974) 272.
[31] O. Dym, M. Mevarech, J.L. Sussman, Science 267 (1995) 1344.
[32] F. Frolow, M. Harel, J.L. Sussman, M. Mevarech, M. Shoham, Nat. Struct. Biol. 3 (1996) 452.
[33] K.L. Britton, P.J. Baker, M. Fisher, S. Ruzheinikov, D.J. Gilmour, M. Bonete, J. Ferrer, C. Pire, J. Esclapez, D.W. Rice, Proc. Natl. Acad. Sci. USA 103 (2006) 4846.
[34] D. Madern, C. Pfister, G. Zaccai, Eur. J. Biochem. 230 (1995) 1088.
[35] D. Madern, C. Ebel, M. Mevarech, S.B. Richard, C. Pfister, G. Zaccai, Biochemistry 39 (2000) 1001.
[36] D. Madern, C. Ebel, G. Zaccai, Extremophiles 4 (2000) 91.
[37] G. Böhm, R. Jaenicke, Prot. Eng. 7 (1994) 213.